Machine Learning — Could It Help in the RIGVIR Case?

Manfred Sneps-Sneppe
Ventspils University of Applied Sciences
Venspils, Latvia
manfreds.sneps@gmail.com

Dmitry Namiot
Lomonosov Moscow State University
Moscow, Russia
dnamiot@gmail.com

***Abstract*— Oncolytic viral therapy is a promising approach to cancer treatment. The first oncolytic virus in the world was the genetically unmodified ECHO-7 strain enterovirus RIGVIR, which was approved in Latvia in 2004 for the treatment of skin melanoma. Our goal is to understand – how could Machine Learning help in the RIGVIR treatment administration. Machine learning for skin disease may well be transferred to practice. Digital image analysis and melanoma genomics studies are promising approaches, but they are currently in their infancy. Machine learning saves time for doctors, but unfortunately does not increase the amount of knowledge about melanoma, since the computer-generated features are difficult to interpret. The analysis shows that the possibilities of classical Linear Discriminant Analysis (LDA) have been successful for cancer diagnostics, but til now it has not been applied to RIGVIR studies. The promising future work is to develop decisive rules in the form of LDA for diagnosing the stages of melanoma during treatment with RIGVIR on the basis of measurements of $CD4^+$, $CD8^+$, and $CD38^+$ lymphocytes and/or their ratios.**

I. Introduction

A) On the oncolytic virus therapy

Oncolytic virus therapy is a novel approach in the field of cancer treatment. First, oncolytic viruses can occur naturally. They can also be created using genetic engineering. The virotherapy method is based on the selective effect of viruses on tumor cells, causing their death or oncolysis, practically without damaging healthy cells and at the same time stimulating normal immunity and its resistance to the tumor (Fig. 1).

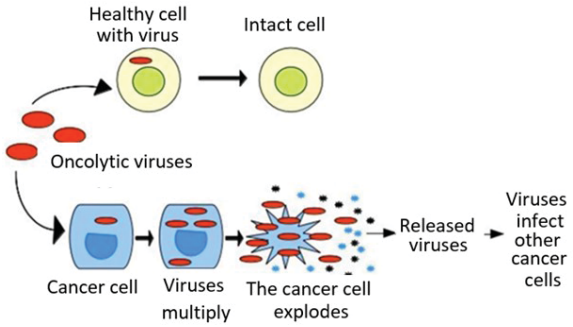

Fig. 1. Schematic representation of oncolytic virotherapy. Viruses can specifically infect cancer cells and then multiply until the cancer cells burst. The newborn viruses are then released to infect (and then burst!) other cancer cells.

Only four oncolytic viruses are registered now (Table I). The first oncolytic virus in the world was the genetically unmodified ECHO-7 strain enterovirus RIGVIR, which was approved in Latvia in 2004 for the treatment of skin melanoma. All other three viruses mentioned in Table I are genetically modified ones [1]. Therefore, RIGVIR is some kind of miracle of nature.

TABLE I. APPROVED ONCOLYTIC VIRUSES UP TO 2021 [1]

Year	Oncolytic virus	Type of tumor
2004	ECHO-7 Rigvir (Latvia)	melanoma
2005	H101 (China)	late-stage refractory nasopharyngeal cancer
2015	T-VEC (USA)	advanced melanoma
2021	Teserpaturev (Japan)	malignant glioma

B) On the history of RIGVIR

In 1960, a previously unknown phenomenon in the world was recorded, namely, that human intestinal viruses (enteroviruses of the ECHO group) obtained from young children are able to destroy certain types of human tumors (angiosarcomas) vaccinated in hamsters [2]. The research started in Latvia in 1959. About 60 types of viruses were isolated from the gastrointestinal tract of healthy children. One of these viruses turned out to be the most suitable for oncology. The first clinical trial was approved in April 1968. The major part of the RIGVIR pre-registration clinical studies was performed during the period from 1968 to 1991. The first oncolytic genetically unmodified ECHO-7 strain enterovirus RIGVIR was approved in Latvia in 2004 for the treatment of skin melanoma.

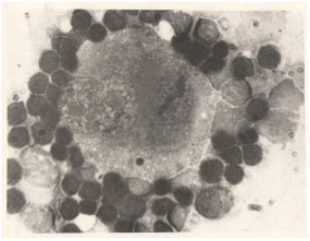

Fig. 2. Melanoma cell surrounded by lymphocytes (RIGVIR therapy) [2].

RIGVIR activates immune cells (lymphocytes) — T-cells and B-cells (Fig. 2). T-lymphocytes occur in the thymus and determine cellular immunity, including the ability to fight intracellular microorganisms, bacteria, viruses, protozoa, and fungi, with transplanted organs. The development of B-lymphocytes occurs in the bone marrow. B-lymphocytes are involved in the body's immune response. RIGVIR administration was based on the changes in $CD4^+$, $CD8^+$, and $CD38^+$ lymphocytes [3]. However formal decisive rules for

differential diagnosis of melanoma stages based on the leukocyte formula remained undeveloped (due to lack of money after the collapse of the Soviet Union).

In March 2019, the distribution of RIGVIR in Latvia was stopped by the State Agency of Medicines, after laboratory tests found that the amount of ECHO-7 virus was in much smaller amounts than claimed. Note, that the virus RIGVIR in the form of injectable medicine is still successfully used these days in the treatment of various cancer types and prevention of metastasis, as well as by people with increased cancer risks.

A new application of RIGVIR is announced in 2023 in the form of the biologically active food supplement RIGVIR SE [4]. It is the world's first food supplement with a unique formula containing a live, adapted, non-pathogenic, and non-genetically modified virus (on the market on the 1st of July, 2023). Rigvir SE contains Vitamin B2, whey protein isolate, and traces of a lyophilized non-genetically modified, and non-pathogenic ECHO-7 virus Rigvir. Rigvir SE is manufactured in the European Union in GMP facilities according to the best pharmacy practices.

C) Melanoma

Melanoma is a type of cancer that develops from pigment-producing cells (Fig. 3). Melanoma is known as the most dangerous and deadly type of skin cancer. It is a highly complex disease characterized by genetic mutations and an immune microenvironment that favors drug resistance and disease progression. Melanoma accounts for approximately 1% of skin cancer but it originates up to 60% of deaths from cutaneous malignancies. At the moment, the main means of evaluating the effectiveness of melanoma treatment is the analysis of leukocytes.

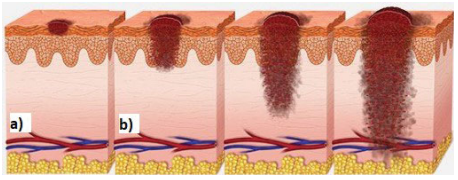

Fig. 3. a) Melanoma starts from pigment-producing cells, b) three stages of melanoma, in the third stage it produces metastases [5].

The remainder of the article is structured as follows. Section II deals with machine learning for melanoma treatment (skin disease diagnoses, digital image analysis, and melanoma genomics) and how to interpret machine learning features. In section III, we look at linear discriminant analysis for the automation of diagnoses and discuss how to apply it to RIGVIR-assisted melanoma treatment on the basis of immune response to melanoma. Section IV is devoted to the conclusion.

II. On Melanoma Treatment

A) On artificial intelligence

Machine learning (ML) is an approach to solving problems by helping machines 'discover' their 'own' algorithms, without needing to be explicitly told what to do by any human-developed algorithms [6]. Deep learning is a type of machine learning in which artificial neural networks (algorithms that are supposed to work like a human brain) are trained on large amounts of data. (Fig. 9). The popularity of such methods is due to their ability to recognize complex patterns in heterogeneous data. Google Scholar gives 76,500 results on the question “Artificial intelligence and melanoma”.

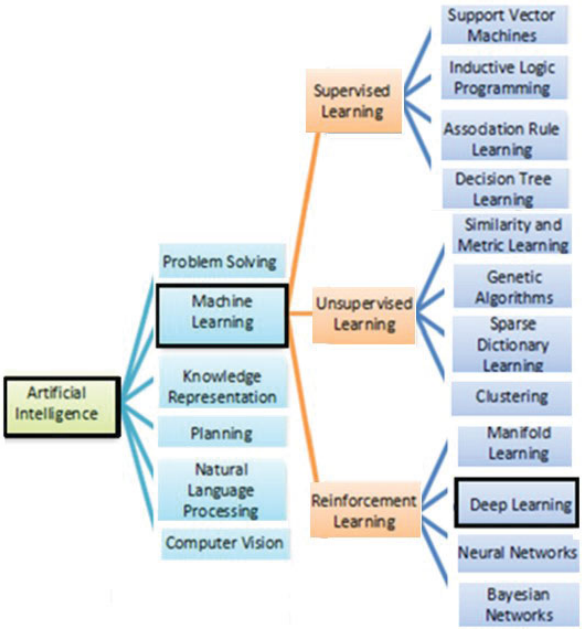

Fig. 4. Machine learning is the heart of artificial intelligence, and its more promising research area is represented by deep learning [6].

The main idea of machine learning is that the patterns that the model has learned (generalized) at the training stage will apply to the entire population, and the model will work successfully with data that was not in the training set. But for many areas, working with a "black box" is not enough or impossible at all (and medicine is the first example here). Accordingly, it is also necessary to interpret what the model has learned. However, this increased focus on explanations has led to considerable confusion about the concept of interpretability. There are many methods of interpretation, and they can often contradict each other.

B) Machine learning for skin disease diagnoses

In [7], deep learning and traditional artificial intelligence machine learning algorithms were applied to use different feature extraction methods to obtain diagnostic accuracy in the early detection of melanoma. To develop a recognition system for detecting skin diseases, the PH2 dataset was used (Fig. 5).

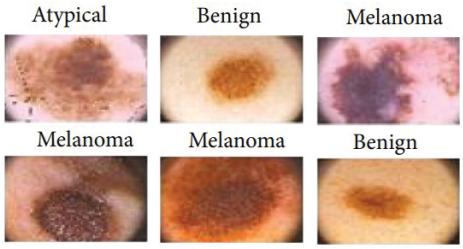

Fig. 5. Images extracted from the PH2 database (benign = noncancerous) [7].

The PH2 dataset is real dermoscopy images; it was used to evaluate the performances of the proposed system for the classification of skin diseases. In studies, 120 dermoscopy

images were considered, and it is divided into 40 atypical nevi, 40 melanoma, and 40 common nevi. The total equaled 120 dermoscopy images; the dataset was divided into 80% training and 20% testing. Figure 5 shows the sample of the PH2 dataset. The PH2 dermoscopy images are JPG format. The resolution of the images is 766 × 560 (428,960 pixels).

The feature-based system was developed based on feature-extracting methods (Fig. 6). In order to segment the lesion from dermoscopy images, the active contour method was proposed. These skin lesions were used to extract features of texture.

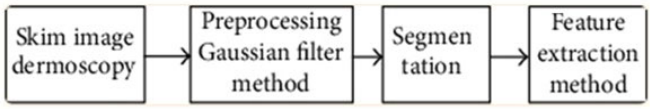

Fig. 6. The steps of skin disease detection by feature extraction [7].

The GLCM (Gray Level Co-occurrence Matrix) method is one of the most powerful statistical extraction feature methods. The GLCM method is used to extract the texture features from dermoscopy images. There are 13 features: energy, contrast, homogeneity, etc. The features of GLCM could be fused with LBP (Local Binary Pattern – another method) to obtain robust features. As a result, 216 significant features were selected for training the classification algorithms (Fig. 7).

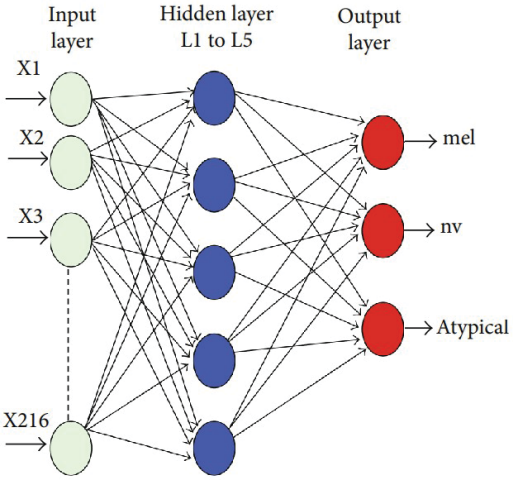

Fig. 7. The architecture of ANN using PH2 [7].

The obtained features were then processed using the artificial neural network (ANN) algorithm. The ANN model achieved an extra high accuracy (98.35%). These results (distinguishing melanoma from other forms of skin diseases) may well be transferred to practice

Note 216 uninterpretable features were used for classification. Excellent results have been achieved in the diagnosis of skin diseases. They can certainly speed up the work of doctors (like how an excavator works faster than a man with a shovel). Does it have any value for physician education? Unfortunately, the doctor is unable to understand these 216 computer-generated signs.

C) Note on interpretable machine learning

The definition of interpretive machine learning (IML) is absolutely clear — it is the ability to get an explanation for the results of the model. Why exactly such a decision was made, what initial data explains it, etc? The study of Interpretable Machine Learning is an extremely hot topic nowadays. Google Scholar gives 277,000 results on this question. We refer to one of the novel methods [8].

In scientific modeling, there is a paradigm that many models implicitly follow. In [8], it is called the paradigm of elementwise representation (ER). A model is ER-type if all model elements (variables, relations, and parameters) represent an element in the phenomenon (components, dependencies, properties). ML Models are not ER-type.

Running example: Classical approach. Suppose a researcher wants to study what attributes influence students' grades in mathematics. He can start with a classical ER model — a linear model with one predictor and one target variable. He selects the student grade in language X_p and in mathematics Y as his proxy variables for students' language and math skills respectively. (In the paper [8], authors use a grading scheme, the range is 0-20, where 0 is the worst and 20 is the best grade.) We assume that the true relationship can be described as $Y = \beta_0 + \beta_1 X_p + \varepsilon$ and an error $\varepsilon \sim N(\mu, \sigma^2)$ and obtain the prediction model that minimizes the mean-squared error (MSE). E.g., it is some like this:

$$m(x_p) = 10.46 + 0.77X_p$$

Our model is ER: we can interpret $\beta_0 = 10.46$ as the predicted math grade for an average student and $\beta_1 = 0.77$ as the strength of association between the language grade and the math grade. In such a simple case, it is easy to explain how the model works, using, for example, 95% confidence intervals for the estimated parameters.

Running example: Artificial Neural Network (ANN). At some point, the linear model will no longer suit us and we can decide to choose a neural network to predict math grades using all the available features. The formal description of the 3 layers model, in this case, looks like this:

$$m_{ANN}(x) = \sigma_3(W_3\sigma_2(W_2\sigma_1(W_1x + b_1) + b_2) + b_3)$$

where model elements are the values of the weight matrices W_1, W_2, W_3 and bias vectors b_1, b_2, b_3, and the activation functions σ_1, σ_2, σ_3. Unlike in the linear model above, it is highly unclear what these parameters correspond to in our data or phenomenon.

In the example discussed above (Fig. 7) with 216 features and 7 levels, the number of computer-generated coefficients becomes incredibly complex and uninterpretable.

D) Digital image analysis of melanoma

In breast cancer, the International TIL working group has put serious efforts into the standardization of TILs scoring and published a guideline that is made for the visual evaluation of HE sections by pathologists. A similar solution should work for melanoma too. Tumor-infiltrating lymphocytes (TIL) have prognostic significance in many tumor types. TIL is a polymorphic group that is composed mainly of effector T lymphocytes, regulatory T lymphocytes, natural killer (NK) cells, dendritic cells, and macrophages.

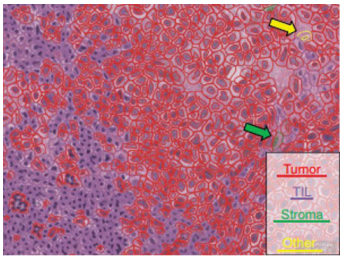

Fig. 8. Representative picture of a sample melanoma case. Using the NN192 algorithm, segmentation shows red indicates tumor cells, purple marks immune cells, green corresponds to stromal cells, and yellow indicates others. Large arrows show example cells [9].

In [9], an algorithm is built for image-based, automated assessment of TILs on H&E stained sections in melanoma [9]. Hematoxylin and eosin stain (H&E stain) is one of the principal tissue stains used in histology. For example, when a pathologist looks at a biopsy of a suspected cancer, the histological section is likely to be stained with H&E. The hematoxylin stains cell nuclei a purplish blue, and eosin stains the extracellular matrix and cytoplasm pink, with other structures taking on different shades, hues, and combinations of these colors. In order to classify detected cells into classes, e.g. tumor cells, immune cells, stromal cells, etc., it used a neural network-based classifier NN192 (Fig. 8). Technically, it is an artificial neural net with eight hidden layers. The NN192 algorithm was applied to every field of view on whole-slide images.

Note that the results of the NN192 algorithm used for H&E stain analysis widely used in histology are impossible to implement widely in medical practice.

E) On melanoma genomics and deep learning

The rapid production and easy access to genomics data have created an unprecedented opportunity to study cancer biology. However, multidimensional data poses a huge challenge for data analysis. The paper [10] identified four genomic clusters using a multimodal neural network with an autoencoder on the dataset from the Cancer Genome Atlas for 8646 patients with 29 cancer types.

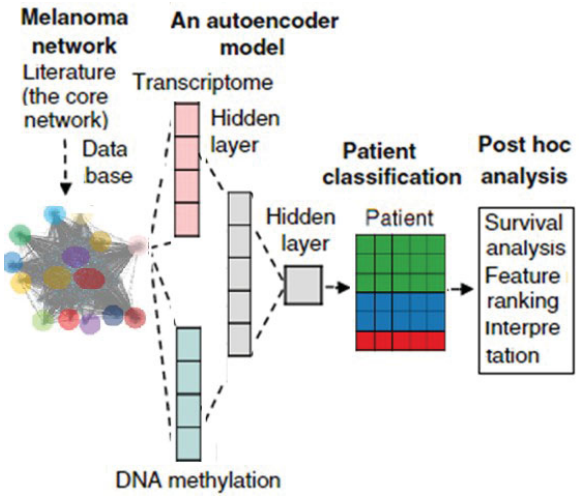

Fig. 9. Integration of The Cancer Genome Atlas data into a melanoma network and performed community identification in the network [11].

In [11], an integrative approach that combines genomic data, a disease network, and a deep learning model to identify and analyze subtypes of melanoma patients is developed. The genomics data of melanoma have high dimensionality, are noisy, and contain sparse signals, which makes them difficult to use.

Figure 9 shows the schema of a machine-learning technique [11]. The genomic profiles were input to the autoencoder model, which converts the genomic data into a score. The resulting melanoma network contains 5860 molecules and 14494 interactions. The integration of genomics data into the network resulted in approximately 20,000 nodes with (1) transcriptome data, (2) DNA methylation data, (3) somatic mutation data, and (4) copy number variation (Table II). As a result, three subgroups of melanoma patients were identified, characterized by different molecular characteristics and different predictions of consequences.

TABLE IV. OVERVIEW OF THE GENOMICS DATA [11]

Category	No. of gene symbols	No. of nodes
Transcriptome (gene expression)	55 500	4983
DNA methylation	33 487	5193
Somatic mutation	19 303	5015
Copy number variation	19 059	4952

The rapid production and easy access to genomics data have created an unprecedented opportunity to study cancer biology. However, multidimensional data poses a huge challenge for data analysis. The studied example shows that melanoma genetic research has a very long way to medical practice.

F) Remarks on artificial intelligence

The above-discussed three cases of melanoma studies:

machine learning for skin disease diagnoses,

digital image analysis,

and melanoma genomics

have illustrated obvious difficulties in bringing these results to medical practice. At least, artificial intelligence approaches are not possible today to propose some practically accessible means for differential diagnostics for melanoma treatment administration.

For more cases see the retrospective review [12]: artificial intelligence methods for the classification of melanoma have been studied extensively. However, few studies compare these methods under the same standards. The performance of traditional machine learning is satisfactory for the small data set of melanomas dermoscopic images, and the potential for deep learning in the future big data era is enormous.

In our opinion, machine learning algorithms for melanoma studies are for the future, nowadays a Linear Discriminant Analysis (LDA) having a long history of development seems more promising.

III. Discriminant Analysis for Automation of Diagnoses

A) On machine learning vs discriminant analysis

The quest for scholarly articles on machine learning vs discriminant analysis gives 114,000,000 results. Linear Discriminant Analysis (LDA) is considered to be a very simple and effective method, especially for classification techniques. LDA is a dimensionality reduction technique. It is used as a pre-processing step in Machine Learning and applications of pattern classification. The goal of LDA is to project the features in a higher-dimensional space onto a lower-dimensional space in order to avoid the curse of dimensionality and also reduce resources and dimensional costs.

The original LDA technique was developed in the year 1936 by Ronald A. Fisher and described as a two-class technique. The multi-class version was later generalized by C.R. Rao as Multiple Discriminant Analysis in 1962.

B) How does Discriminant Analysis work?

We apply Multidimensional Discriminant Analysis. It is some kind of logistic regression analysis based on the use of linear discriminant functions (LDF):

$$F = w_1x_1 + w_2x_2 + \ldots + w_mx_m$$

This record $x_1, x_2, \ldots, x_m$ denotes the symptoms (signs) which in each specific case, i.e., certain numerical values are assumed for each patient; $w_1, w_2, \ldots, w_m$ — coefficients that include the diagnostic value of symptoms; m — the number of symptoms (usually tens or even hundreds). Qualitative symptoms that may correspond to the statements «white» or «black» should be coded with numbers, for example, «white» = 0, «black» = 1

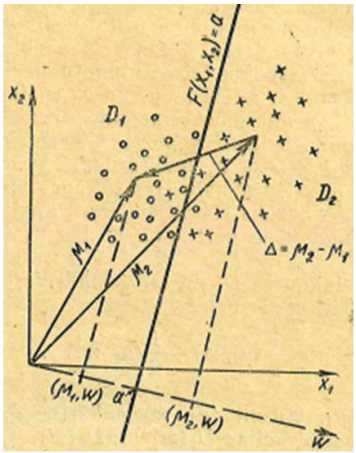

Fig. 10. Construction of LDF for two symptoms.

The following geometric interpretation can be given to the discriminant function and the decision-making process itself (Fig. 10). Let's start with two symptoms x_1 and x_2, say, temperature and blood pressure because then everything can be represented graphically. So, when measuring the symptoms x_1 and x_2, one of two decisions must be made D_1 or D_2. To do this, you need to know the numerical value of the discriminant $F = w_1x_1 + w_2x_2$, i.e., one should know the coefficients w_1 and w_2, as well as the decision parameter a. From where to take the numerical values size as well w_1 and w_2 and the parameter a? They are obtained by processing medical histories (or polyclinic outpatient cards), which show not only symptom values but also a diagnosis reliably established, for example, after surgery. Therefore, N_1 medical histories with a diagnosis D_1 and N_2 histories D_2 with a diagnosis should be taken. Each of the histories for two symptoms can be represented by a point on the plane.

In Fig. 10, every diagnosis D_1 case is represented by a circle, diagnosis D_2 case — by a cross. If patient groups are represented geometrically, they are usually grouped by diagnosis. The discriminant function F, which is a straight line $w_1x_1 + w_2x_2 = a$, divides the plane into two parts. The equation of the straight line should be chosen in such a way as to separate the groups of patients from each other as best as possible. In the picture, μ_1 and μ_2 are the vectors that indicate the centers of "gravity" of patient groups, w — the vector of diagnostic coefficients. Geometrically, any line $F = w_1x_1 + w_2x_2$ is perpendicular to the vector w. Of all these lines, the one that best divides the sets must be chosen. It also determines the cutoff number a. The points (μ_1, ω) and (μ_2, ω) correspond to the projections of the centers of gravity of the clusters onto the vector w. If both diagnoses are equally probable, then the midpoint of the value $\Delta = \mu_2 - \mu_1$ can be taken as the decision parameter.

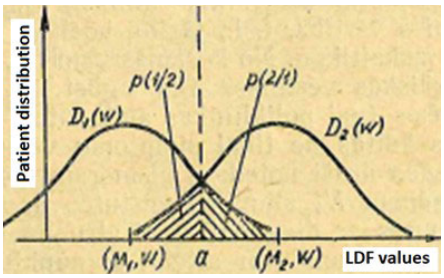

Fig. 11. Distribution of numerical values of LDF and selection scheme of diagnoses D_1 and D_2

Projections of patient groups $D_1(w)$ and $D_2(w)$ are grouped around points (μ_1, ω) and (μ_2, ω). This is shown in the picture (Fig. 11), from which it is clear what it means to decide D_1 or D_2. Let's say a patient comes to the polyclinic. The doctor or nurse determines the symptom values x_1^0 and x_2^0 and enters them into the computer. If $w_1x_1 + w_2x_2 < a$, i.e., the point (x_1^0, x_2^0) is to the left of the line $w_1x_1 + w_2x_2 = a$, then the computer writes the diagnosis D_1, if $w_1x_1 + w_2x_2 > a$, then — the diagnosis D_2. The underlined areas in the figure show diagnosis errors: $p(1/2)$ — the probability of accepting the diagnosis D_1 under the condition that the correct diagnosis is D_2; $p(2/1)$ — on the contrary.

A similar geometrical interpretation can be given in the general case of m symptoms. In this case, the mathematical formulas become more complicated. But it is important to note a very important fact, that is, even in the case of m symptoms, the decision-making scheme does not change. Two m-dimensional clouds are divided by plane. The line

$$w_1x_1 + w_2x_2 + \ldots + w_mx_m = a$$

pass through the middle point of the centers of two m-dimensional clouds and their projections are separated by point a.

C) Cancer diagnostics

Let us give a few examples from our own medical practice referring to the period 1965-1978 [13]. The work was carried out in the Mathematical Methods Laboratory of the All-Union Institute of Medical Apparatus Construction (Moscow). Medical data was taken from the P.A. Hertzen Moscow Oncology Research Institute's database and the research work was done in cooperation with the named institute.

Breast cancer. Mammography is an X-ray imaging technique used to examine the breast for early detection of cancer and other diseases. A radiologist will carefully examine a mammogram (Fig. 12) to search for high-density regions or areas of unusual configuration that look different from normal tissue. Radiologists examine precisely abnormal areas. The defining parameters for them are usually the size, shape, and contrast of each anomalous area. The appearance of the edges or margins of such an area also matters. All of these signs may indicate the possibility of a malignant neoplasm (cancer).

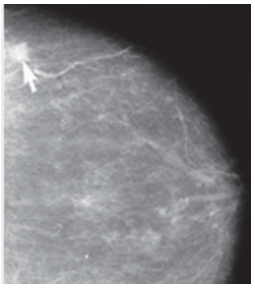

Fig. 12. A mammogram showing a small cancerous lesion. It is hard to find cancer in conditions of routine doctor's work.

In another similar case, 1,100 verified medical histories were treated (550 cancers and 550 non-cancers). These were only conclusions made on fluorograms, when the presence of opacities in the lungs, the contours and contrast of opacities, etc. were evaluated. The nurse reviewed each fluorogram and entered into the card 33 signs characterizing the fluorogram. Of these features, only 11 are informative enough to give 90% correct diagnoses when tested against real case histories. (Fig. 13). This is the level of correct diagnosis that a highly qualified doctor achieves. But — the formulation of such diagnoses takes a lot of time. Any restrictions on the doctor's work time lead to an increase in the number of errors. The main conclusion is that a nurse using a computer can achieve the accuracy of diagnoses of a highly qualified unhurried doctor.

Let us note an important fact of statistical analysis, that is, the number of informative symptoms depends on the amount of data. It turned out that using all 33 features, the percentage of correct diagnoses decreased by 3-4%. It turned out that the number of informative signs is three times smaller — only 11 signs. The number of informative features increases by increasing the number of patients (more than 1000 case histories).

Lung cancer. The P.A. Hertzen Moscow Oncology Research Institute developed an X-ray examination map for the diagnosis of peripheral lung cancer. Statistical analysis, first of all, showed that out of 82 signs (answers to questions) and 240 symptoms of the disease, it is enough to leave 28 signs and 76 symptoms, i.e. 32% of the original data set. Second, and more importantly, a nurse can fill out a medical chart and receive a diagnosis from a computer without the involvement of a doctor, and this diagnosis turns out to be much more accurate than the decision of a radiologist (Fig. 14).

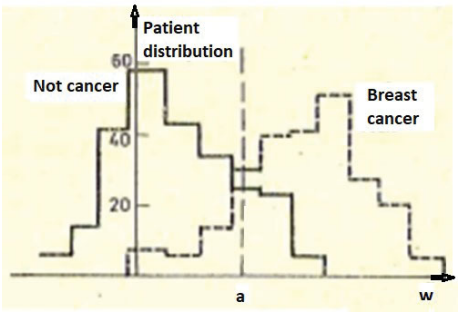

Fig. 13. Distribution of LDF numerical values in 550 cancer and 550 non-cancer cases (1000 case histories).

The use of the LDF approach provided 87.8% of correct diagnoses compared with 65% of correct radiologist diagnoses (Table III).

Fig. 14. A chest X-ray showing a tumor in the lung (marked by arrow).

TABLE III. HOW COMPUTERS CAN IMPROVE DIAGNOSTIC ACCURACY

Diagnostic result	Computer diagnosis	Radiologist diagnosis
Correct answer	87.8%	65%
Wrong answer	4.4%	10%
Refusal to diagnose	7.8%	25%

Concluding the discussion of multivariate statistical analysis, we note that, 50 years ago, in the case histories, there were features (signs) that were understandable to a person, that is, to the human eye, ear, and other sense organs. The machine learning program, on the other hand, describes diseases with signs that differ from human perception. Even more difficult, different machine learning programs can describe diseases in uninterpretable features.

D) Modeling of immune response

As mentioned above, RIGVIR administration was based on the changes in $CD4^+$, $CD8^+$, and $CD38^+$ lymphocytes [3].

In reality, the immune response to cancer cells is very complex [14]. The natural defense against germs is the innate immune system. Its main components are:

(1) Epithelium (physical protection) and antimicrobial chemicals formed on the surface of the epithelium (chemical protection);
(2) Phagocytic cells (neutrophils, macrophages), dendritic cells, natural killer (NK) cells, and other innate lymphoid cells;
(3) Blood proteins.

Several therapeutic strategies to inhibit melanoma growth have specifically focused on the activation of the anti-tumor activities of naive or differentiated innate subsets found within tumors. Functional effector T cells must be recruited to melanomas through a chemokine gradient (CXCL9, CXCL10, CXCL11) generated by dendritic cells (DC) or tumor-associated stroma.

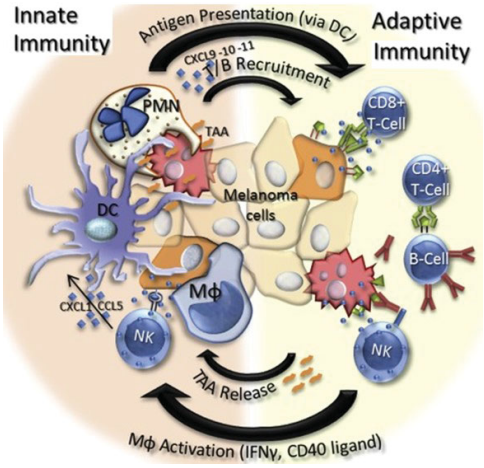

Fig. 15. Melanoma Clearance by Functioning Immune Cells [14].

The key interactions of immune cells (Fig. 15):

- In innate immunity, natural killer (NK) cells bind tumor cells via receptor/ligand interactions and release cytolytic molecules causing tumor cell death.
- Phagocytes engulf dead tumor cells, process and present tumor-associated antigens (TAA). Phagocytes include dendritic cells (DC), polymorphonuclear neutrophils (PMN), and macrophages (Mφ).
- DCs are actively recruited by cytokines (CXC) secreted from activated NK cells.
- Recruitment of T- and B-lymphocytes by chemokine gradients and presentation of TAAs to T- and B-cells activates the adaptive immunity.
- Tumor-specific CD8 + T-cells bind tumor cells presenting TAA on MHC molecules via engagement of the T-cell receptor, leading to the release of cytotoxic granules into tumor cells.
- Tumor-specific CD4 + T-cells engage B-lymphocytes via TAAs presented by MHC molecules leading to the release of antibodies specific for TAAs whose binding causes tumor cell death.
- Adaptive immune cells also re-activate innate immunity through receptor/ligand interaction as well as cytokine release.

The picture of immune cell interaction against tumors is extremely complex. Currently, there are only preliminary ideas about the growth of the immune response in melanoma.

D) On future work

First of all, it would be necessary to develop decisive rules in the form of LDF for diagnosing the stages of melanoma during treatment with RIGVIR on the basis of measurements of $CD4^+$, $CD8^+$, and $CD38^+$ lymphocytes and/or their ratios, which are set out in [3]. Note that this is a huge amount of work requiring thousands of experimental animals infected with melanoma and treated with RIGVIR.

In parallel, other immune responses should be studied, e.g., a chemokine gradient (CXCL9, CXCL10, CXCL11), and so on.

IV. Conclusion

Oncolytic viral therapy is a promising approach to cancer treatment. The first oncolytic virus in the world was the genetically unmodified ECHO-7 strain enterovirus RIGVIR, which was approved in Latvia in 2004 for the treatment of skin melanoma. Therefore, RIGVIR is some kind of miracle of nature.

Our goal is to understand – how could Machine Learning help in the RIGVIR treatment administration. There are two issues: (1) to detect melanoma between other skin diseases, (2) to separate several melanoma stages. Machine learning for skin disease (distinguishing melanoma from other forms of skin diseases) may well be transferred to practice. Digital image analysis and melanoma genomics studies are promising approaches, but they are currently in their infancy. Besides, machine learning saves time for doctors, but unfortunately does not increase the amount of knowledge about melanoma, since the computer-generated diagnostic features are difficult to interpret. The potential of artificial intelligence (machine learning) is obvious, but its application in oncology is still in its early stages and far from being fully clinically tested [15].

The analysis shows that the possibilities of classical Linear Discriminant Analysis (LDA) have been successful for cancer diagnostics, but til now it has not been applied to RIGVIR-assisted melanoma treatment in different stages of disease.

The main means of evaluating the effectiveness of melanoma treatment remains the analysis of leukocytes, as in the days of the oncolytic virus RIGVIR discoverer, Aina Muceniece (1924 – 2010) [3]. The promising future work is to develop decisive rules in the form of LDA for diagnosing the stages of melanoma during treatment with RIGVIR on the basis of measurements of $CD4^+$, $CD8^+$, and $CD38^+$ lymphocytes and/or their ratios. Note that this is a huge amount of work requiring thousands of experimental animals infected with melanoma and treated with RIGVIR.

ACKNOWLEDGMENT

We would like to thank the reviewers for many helpful remarks. Unfortunately, it was not possible to supplement the article with a number of recommended additions, which required a significant expansion of the scope of the article.

REFERENCES

[1] Bifulco, M., Zazzo, E.D., Napolitano, F., et al. “History of how viruses can fight cancer: From the miraculous healings to the approval of oncolytic viruses”. *Biochimie.* Vol 206, March 2023, 89-92 https://doi.org/10.1016/j.biochi.2022.10.008

[2] Alberts, P., Tilgase, A., Rasa, A., et al. “The advent of oncolytic virotherapy in oncology: The Rigvir story”. *European Journal of Pharmacology*. Vol 837, 15 Oct 2018, 117-126. https://doi.org/10.1016/j.ejphar.2018.08.042

[3] Muceniece, Aina, and Venskus, Dita. *How to assess immunity (melanoma model).* Riga, 2007 (in Latvian).

[4] Biologically active food supplement RIGVIR SE. Web: https://www.smartnanovirus.com/

[5] Web: Stages of Melanoma Skin Cancer (everydayhealth.com).

[6] Guerrisi, A., Falcone, I., Valenti, F., et al. “Artificial Intelligence and Advanced Melanoma: Treatment Management Implications”. *Cells* **2022**, *11*, 3965, doi.org/10.3390/cells11243965.

[7] Alsaade, F.W., Aldhyani, T.H.H., Al-Adhaileh, M.H. “Developing a Recognition System for Diagnosing Melanoma Skin Lesions Using Artificial Intelligence Algorithms”. *Comput Math Methods Med*. 2021 May 15; 2021:9998379. Doi: 10.1155/2021/9998379.

[8] Freiesleben, T., König, G., Molnar, Ch., Tejero-Cantero, A. “Scientific Inference with Interpretable Machine Learning: Analyzing Models to Learn About Real-World Phenomena”. June 2022. Web: https://doi.org/10.48550/arXiv.2206.05487

[9] Acs, B., Ahmed, F.S., Gupta, S., et al. “An open-source automated tumor-infiltrating lymphocyte algorithm for prognosis in melanoma”. *Nat Commun* **10**, 5440 (2019). Web: https://doi.org/10.1038/s41467-019-13043-2

[10] Xie F., Zhang J., Wang J., et al. “Multifactorial deep learning reveals pan-cancer genomic tumor clusters with distinct immunogenomic landscapes and responses to immunotherapy”. *Clin Cancer Res*. 2020; 26(12): 2908-2920.

[11] Lai, X., Zhou, J., Wessely, et al. “A disease network-based deep learning approach for characterizing melanoma”. *International Journal of Cancer*. 150, 6, p. 1029-1044. 15 Mar 2022.

[12] Cui, X., Wei, R., Gong, L., et al. “Assessing the effectiveness of artificial intelligence methods for melanoma: A retrospective review”. *Journal of the American Academy of Dermatology.* 2019; 81 (5). Web: doi.org/10.1016/j.jaad.2019.06.042.

[13] Sneps-Sneppe, M. A. *Mathematics, and Health Care.* Moscow, 1982 (in Russian).

[14] Marzagalli, M., Ebelt, N.D., Manuel, E.R. “Unraveling the crosstalk between melanoma and immune cells in the tumor microenvironment”. *Seminars in Cancer Biology*. Vol 59, Dec 2019, 236-250. Web: https://doi.org/10.1016/j.semcancer.2019.08.002

[15] Yin, J.; Ngiam, K.Y.; Teo, H.H. “Role of Artificial Intelligence Applications in Real-Life Clinical Practice: Systematic Review*”. J. Med. Internet Res*. 2021, 23, e25759.